Glassy dynamics in the asymmetrically constrained kinetic Ising chain

P. Sollich[1] and M. R. Evans[2]
[1]*Department of Mathematics, Kings College London, Strand, London WC2R 2LS, United Kingdom*
[2]*School of Physics, University of Edinburgh, Mayfield Road, Edinburgh EH9 3JZ, United Kingdom*
(Received 18 March 2003; published 26 September 2003)

We study the dynamics of the East model, comprising a chain of uncoupled spins in a downward-pointing field. Glassy effects arise at low temperatures T from the kinetic constraint that spins can only flip if their left neighbor is up. We give details of our previous solution of the nonequilibrium coarsening dynamics after a quench to low T [Phys. Rev. Lett. **83**, 3238 (1999)], including the anomalous coarsening of down-spin domains with typical size $\overline{d}\sim t^{T\ln 2}$, and the pronounced ''fragile glass'' divergence of equilibration times as $t_*=\exp(1/T^2\ln 2)$. We also link the model to the paste-all coarsening model, defining a family of interpolating models that all have the same scaling distribution of domain sizes. We then proceed to the problem of equilibrium dynamics at low T. Based on a scaling hypothesis for the relation between time scales and length scales, we propose a model for the dynamics of ''superdomains'' which are bounded by up-spins that are frozen on long time scales. From this we deduce that the equilibrium spin correlation and persistence functions should exhibit identical scaling behavior for low T, decaying as $g(\tilde{t})$. The scaling variable is $\tilde{t}=(t/t_*)^{T\ln 2}$, giving strongly stretched behavior for low T. The scaling function $g(\cdot)$ decays faster than exponential, however, and in the limit $T\to 0$ at fixed $\tilde{t}$ reaches zero at a *finite* value of $\tilde{t}$.

DOI: 10.1103/PhysRevE.68.031504 PACS number(s): 64.70.Pf, 05.70.Ln, 05.20.−y, 75.10.Hk

I. INTRODUCTION

The phenomenology of glassy systems—see, e.g., Refs. [1–4] for excellent reviews—has inspired many theoretical descriptions and explanations. Experimentally, long relaxation times are observed; when these become much longer than the observation time scale a glass transition is said to occur. Other signatures of glassy dynamics are correlation functions that can be fitted by a stretched exponential decay law and aging phenomena [5] where, since the system is out of thermal equilibrium, it keeps evolving as time goes by and time-translation invariance is broken.

From a modeling perspective the same phenomenology arises when one studies simple model systems by computer simulation. Again, relaxation times can outstrip the time available to run a simulation and one never explores the equilibrium state.

The long relaxation times in glasses typically show a pronounced divergence as the temperature T is lowered and are often fitted experimentally by the Vogel-Tammann-Fulcher (VTF) law

$$\tau=\tau_0\exp[-A/(T-T_0)]. \tag{1}$$

The relaxation time τ may characterize, for example, the time for a density fluctuation or an externally imposed stress to relax. Although some heuristic justifications have been offered [6], for practical purposes VTF is just a fit with three parameters τ_0, A, T_0. For $T_0=0$ it reduces to an Arrhenius law. A system for which T_0 is small, so that one has something close to Arrhenius behavior, is referred to as a ''strong glass,'' whereas a system exhibiting large deviations from Arrhenius behavior is called a ''fragile glass.'' Generally, T_0 is much lower than the experimental temperatures so that the mathematical singularity in the fit (1) is not physically relevant in an experiment. From the theoretical point of view, however, there has been a long debate over whether T_0 might represent a true thermodynamic transition temperature which would in principle be measurable in the limit of infinitely slow cooling.

Although (1) is popular, it is not the only possibility for a fit. For example, the exponential inverse temperature squared (EITS) form

$$\tau=\tau_0\exp(B/T^2) \tag{2}$$

has been proposed as an alternative. This form does not exhibit a singularity at any finite T. Experimentally, or in a computer simulation, it is difficult to distinguish between VTF and EITS behavior due to obvious limitations on the longest accessible time scales; both can represent the experimentally observed $\tau(T)$ in many materials [7]. Theoretical work is thus essential for clarifying whether VTF or EITS might be more appropriate.

Stretched exponential decay of a relaxation function, let us say an autocorrelation $q(t)$, is expressed by the Kohlrausch-Williams-Watt law

$$q(t)\sim\exp[-(t/\tau)^b], \tag{3}$$

where the stretching exponent $b<1$. An heuristic explanation for this law is that there is a broad distribution $\Omega(\tau)$ of relaxation modes with decay constants τ,

$$q(t)=\int d\tau\,\Omega(\tau)\exp(-t/\tau). \tag{4}$$

For example, if one assumes $\Omega(\tau)\sim\exp(-a\tau)$ then for large t the dominant modes have $\tau=(t/a)^{1/2}$ which leads to Eq. (3) with $b=1/2$. This however leaves the physical mechanisms by which such a relaxation time distribution would arise unclear.

One idea proposed to generate a broad distribution of relaxation times from an explicit dynamical model was that of a hierarchy of degrees of freedom [8]. The different levels in the hierarchy then relax in series, the degrees of freedom in one level having to wait for the degrees of freedom in the level below to reach some configuration before they are free to evolve. This latter condition is a realization of a *kinetic constraint*.

A more concrete realization of a kinetic constraint is the *f*-spin facilitated kinetic Ising model introduced by Fredrickson and Andersen [9]. Here no hierarchical structure needs to be posited by hand to generate slow dynamics. All microscopic degrees of freedom are of the same kind, namely, noninteracting Ising spins on a simple cubic lattice in a downward-pointing field. However a spin can only flip if at least f nearest neighbor spins are pointing up (against the field). For $f \geqslant 2$ this gives rise to slow cooperative relaxation, as reviewed in, e.g., Ref. [10]. The physical motivation for the kinetic constraint in this model becomes clear if one thinks of the spins as coarse-grained density variables in a supercooled liquid, with up- and down-spins corresponding to low- and high-density regions. The constraint then states that a change in local density is only possible if the overall density in the surrounding regions is low enough for the particles to be able to rearrange.

An interesting modification of the Fredrickson-Andersen model arises when the kinetic constraints are made anisotropic. In the one-dimensional version considered here, called the East model [11], a spin can only flip if its left (west) neighbor is pointing up, so that information propagates only to the east. The rates for flipping mobile spins are 1 for down-flips and $\epsilon = \exp(-1/T)$ for up-flips, giving a small equilibrium concentration $c = \epsilon/(1+\epsilon)$ of up-spins at low T (see Sec. II for details). The number of spins which are mobile because their left neighbor is up will then also be small, and this makes it plausible that the dynamics will slow down dramatically as T decreases.

In this paper we study the glassy dynamics of the East model, both in equilibrium and out of equilibrium. We focus on low temperatures T. This is the regime that is most interesting since glassy features will be most pronounced; it is also the regime where theoretical studies such as ours are most needed, since the extremely long relaxation time scales make numerical simulations difficult or impossible.

Before outlining the structure of this paper, we give a brief review of existing work on the East model. Much research to date has concerned the *equilibrium* dynamics, as encoded, e.g., in relaxation functions such as spin autocorrelation $C(t)$ or persistence $\mathcal{P}_1(t)$ (see Sec. IV A for definitions). Already when the model was first proposed [11] it was argued that relaxation time scales should remain finite for any $T > 0$, thus excluding a transition to a nonergodic state where relaxation functions fail to decay to zero. This has recently been proved rigorously: the longest relaxation time, defined as the inverse of the smallest decay rate that one would find by full diagonalization of the master equation, is bounded between $\exp(1/2T^2 \ln 2)$ and $\exp(1/T^2 \ln 2)$ in the limit of small temperatures [12]. The form of the bounds demonstrates that the East model has EITS behavior; we will find below that it is the upper bound $t_* = \exp(1/T^2 \ln 2)$ that gives the dominant low-T behavior of the relaxation times.

A number of approaches have been used to predict the actual shape of the equilibrium relaxation functions. An ''effective medium approximation'' [11,13] for $C(t)$ leads to a self-consistency equation typical of mode-coupling approximations (MCA) and predicts a spurious nonergodic transition at $c = 0.5$ ($\epsilon = 1$); effectively the same result was later derived using diagrammatic methods [14]. The version of MCA derived by Kawasaki [15] also gives a spurious transition, at $c = 0.2$ ($\epsilon = 1/4$). Both approximations can therefore only be reasonable at sufficiently large ϵ, or for short times at smaller ϵ; a comparison with numerical simulations [16] shows that the effective medium approximation is generally more accurate in these regimes. Improved diagrammatic resummations [14] avoid the prediction of a spurious transition, and are quantitatively more satisfactory over a larger range of t and ϵ. However, for small ϵ they still predict a decay of $C(t)$ that is too fast and too similar to an exponential compared with numerical simulations. The nonexponential behavior of $C(t)$ had been noticed early on [11], but is well fitted by a stretched exponential only over a limited time range. We conjectured in Ref. [17], and will find below, that the correct scaling variable for $C(t)$ at low T is indeed of a ''stretched'' form, $\tilde{t} = (t/t_*)^{T \ln 2}$, but that the relevant scaling function decays more quickly than an exponential. The stretching exponent $T \ln 2$ was also found to govern the decay of the up-spin persistence $\mathcal{P}_1(t)$ [18,19].

Recently, interest in the East model has shifted to more complicated features of the equilibrium dynamics, e.g., the existence of dynamical heterogeneities [20], and to the out-of-equilibrium behavior. In Ref. [21], nonlinear relaxation processes after large changes in T were simulated. Otherwise, interest has centered on the behavior after a quench from high to low temperature. For a quench to exactly $T = 0$, the dynamics is exactly solvable [22,23]. The solution is essentially equivalent to that of the corresponding model with isotropic constraints, i.e., the one-dimensional Fredrickson-Andersen model with $f = 1$ [24,25], and in fact also applies to a whole family of models that interpolate between the isotropic and anisotropic limits [18,19]. For a quench to nonzero T, the autocorrelation function $C(t, t_w)$ between spins at times t_w and t after the quench and the corresponding response were simulated in Ref. [22]. The correlation $C(t, t_w)$ exhibits plateaux, which we will see in Sec. III C can be rationalized from the hierarchical nature of the dynamics. Nonequilibrium steady states caused by applying an external ''drive'' have recently also been studied, using a ''tapping dynamics'' inspired by ideas from granular media [26] as well as ''rheological driving'' designed to model the effect of a shear flow [27]. Finally, we mention an interesting two-dimensional spin model, which can be mapped onto a system of noninteracting defects with kinetic constraints and turns out to have low-T behavior very similar to that of the East model [28–30].

The paper is organized as follows. After defining the East model fully in Sec. II, we turn to the out-of-equilibrium dynamics in Sec. III, giving details of the results announced in

Ref. [17]. After a quench to low temperature, the equilibrium concentration of up-spins at the new T is small compared to its initial value. Thus up-spins are eliminated, essentially irreversibly, and the dynamics can be viewed as a coarsening process whereby down-spin domains coalesce as up-spins disappear. We find the scaling of the rates at which domains of length d disappear, which follow a hierarchical pattern so that the coarsening dynamics splits into well-separated stages. This allows us to find an exact solution for $T\to 0$. The overall scaling of the rates, as $\Gamma(d)\sim d^{-1/T\ln 2}$, also implies that the system exhibits anomalous coarsening, with typical domain sizes increasing with time as $\overline{d}\sim t^{T\ln 2}$. Extrapolating to equilibrium domain lengths $\overline{d}_{\rm eq}\approx 1/\epsilon$ (see below) then gives the dominant divergence of the equilibration time as $t_*\sim\exp(1/T^2\ln 2)$. Interestingly, in the scaling limit of the out-of-equilibrium dynamics ($1\ll\overline{d}\ll\overline{d}_{\rm eq}$), we find that the domain size distribution is identical to that of the paste-all model [31]. We rationalize this observation, and provide in Sec. III D a family of models with identical scaling distributions that interpolate between the paste-all and East model limits.

In Sec. IV we shall then explore the *equilibrium* dynamics. Based on a plausible conjecture regarding the scaling of relaxation times with distance at low T, we introduce a simplified picture which we refer to as the *superdomain model*. This should capture the essence of the equilibrium dynamics and become exact in the $T\to 0$ limit. The model enables us to probe the long time scales of the equilibrium dynamics numerically, and leads us to a scaling form for the equilibrium spin autocorrelation function, $C(t)=g(\tilde{t})$, with $\tilde{t}=(t/t_*)^{T\ln 2}$. This shows strong stretching for $T\to 0$, but it will turn out that the scaling function g decays more quickly than an exponential, actually decreasing to zero at a finite value of $\tilde{t}$. Finally, a brief summary of our results and outlook to future work is given in Sec. V.

II. MODEL DEFINITION

The model comprises L Ising spins $s_i=0,1$ on a one-dimensional lattice with periodic boundary conditions (site $i=L+1$ is identified with site $i=1$). The dynamics are defined by the following spin-flip rates:

$$11\to 10 \text{ with rate } 1,$$

$$10\to 11 \text{ with rate } \epsilon=\exp(-1/T). \tag{5}$$

Thus a spin can only flip if its left neighbor is pointing up (note that in the original paper [11] the mirror image of the above definition was used, so that the *right* neighbor had to point up for a spin to be able to flip). By a rate, say x, we mean that in a small time dt the event happens with probability $x\,dt$. It is easy to check that the dynamics obey detailed balance with respect to the energy function $E=\Sigma_{i=1}^{L}s_i$, i.e., the equilibrium distribution corresponds to free spins in a downwards pointing field:

$$P_{\rm eq}(\{s_i\})=\frac{1}{Z}\exp\left(-\frac{1}{T}\sum_i s_i\right)=\frac{\epsilon^{\Sigma_i s_i}}{(1+\epsilon)^L}. \tag{6}$$

It follows that the equilibrium concentration of up-spins, $c=\langle s_i\rangle$, is given by

$$c=\frac{\epsilon}{1+\epsilon}. \tag{7}$$

To show that this is the unique steady state we require that the (finite) system is ergodic, i.e., that any configuration can be reached from any other. This is true for all configurations except for that with all spins down; this is a configuration that can be neither entered nor left and that we therefore ignore. To see that the rest of the configuration space is ergodic, note that from any configuration with a nonzero number of up-spins one can flip spins up until the ''all up'' configuration is reached. Then, to obtain any desired configuration one flips spins down in an ordered way to create the appropriate regions of down-spins.

The basic objects that we use for the description of the system are *domains*. As shown by the vertical lines in

$$\ldots 0|1000|1|1|10|100|1|1|10|10\ldots,$$

a domain consists of an up-spin and all the down-spins that separate it from the nearest up-spin to the right. (This convention is opposite to that of Ref. [17], but leads to equivalent conclusions and will be more convenient in our treatment of equilibrium dynamics in Sec. IV below.) The length d of a domain then gives the distance between the up-spin at its left edge and the next up-spin to the right. Note that adjacent up-spins are counted as separate domains of length $d=1$. In equilibrium, it follows from Eq. (6) that the domain lengths are geometrically distributed

$$P_{\rm eq}(d)=\epsilon/(1+\epsilon)^d \tag{8}$$

with mean

$$\overline{d}_{\rm eq}=\frac{1+\epsilon}{\epsilon}. \tag{9}$$

As explained, our aim will be to pursue analytical calculations where possible, but we explain briefly how simulations were carried out. We used a continuous-time Bortz-Kalos-Lebowitz (BKL) [32] algorithm, where the time intervals between spin flips are sampled directly; a standard Monte Carlo algorithm where spin flips are first proposed and then accepted or rejected would be much slower at low T. In the BKL algorithm, once the time interval to the next flip is determined one decides probabilistically which of the mobile spins to flip, choosing each with a probability p_i proportional to its flip rate (1 or ϵ). A simple method for doing this would be to sample a uniform random variable r on $[0,1]$ and then go through the mobile spins until the spin i is found for which $\Sigma_{j=1}^{i-1}p_j<r\leqslant\Sigma_{j=1}^{i}p_j$. This search for i takes $O(L)$ steps, however, and in fact for large L quickly becomes the most computationally intensive part of the algorithm. In-

stead, we define partial sums $q_{j,a}$ over all blocks of spins of length 2^a, where $a=0,\ldots,l$ if the total chain length is $L=2^l$. The $q_{j,a}$ can be defined recursively by $q_{j,a=0}=p_j$ and

$$q_{j,a}=q_{2j-1,a-1}+q_{2j,a-1} \quad (j=1,\ldots,L/2^a).$$

(In fact, we work with analogous partial sums for the number of mobile up- and down-spins separately, from which the $q_{j,a}$ can easily be retrieved; this allow us to use fast integer arithmetic.) The $q_{j,a}$ can be thought of as arranged on a binary tree, and finding the spin i to flip becomes a simple walk from the top level $a=l$ to the bottom level $a=0$, branching left or right on each level to keep r within the $q_{j,a}$ values bounding the remaining subpart of the tree. This takes $l\sim\ln L$ steps, and the $q_{j,a}$ can be updated in similar time once a spin has been flipped, giving a reduction in computing time $\sim(\ln L)/L$. Compared to earlier simulations, e.g., Ref. [21], rather longer time scales (up to $t=10^{11}$) can be accessed with this method.

III. NONEQUILIBRIUM DYNAMICS

A. Coarsening dynamics

In this section we consider the dynamics of the East model after a quench from equilibrium at some high initial temperature $T\gg 1$ to low temperature $T\ll 1$ ($\epsilon\to 0$) [17]. At the new temperature the equilibrium concentration of up-spins is much smaller than before, so that the number of up-spins must decrease in time. Correspondingly, the typical domain sizes must grow: the system coarsens.

To understand the nature of this coarsening process, recall first that the equilibrium concentration of up-spins is, from Eq. (7), $c=1/d_{\rm eq}=\epsilon+O(\epsilon^2)$. Hence the equilibrium probability of finding an up-spin within a chain segment of *finite* length d is $O(d\epsilon)$ and tends to zero for $\epsilon\to 0$. In the limit

$$\epsilon\to 0 \text{ at fixed } d, \tag{10}$$

the flipping down of up-spins therefore becomes *irreversible to leading order* [33]. In terms of domains, this means that the coarsening dynamics of the system is one of coalescence of domains: an up-spin that flips down merges two neighboring domains into one large domain. Note that the limit (10) does not extend to include equilibrium domain lengths that scale as $d\sim 1/\epsilon$. Therefore the irreversible coarsening is a purely nonequilibrium phenomenon and does not pertain to the equilibrium dynamics; this is why at low T the former is in fact *easier* to analyze than the latter, as we shall see.

Irreversible coarsening processes such as that above have been studied in a variety of contexts. In particular, if the rate of elimination depends solely on the domain size and not on the sizes of neighboring domains there is a very convenient property: during such a process, no correlations between the lengths of neighboring domains can build up if there are none in the initial state. The proof is an easy generalization of that of Ref. [34]. We include it for completeness here. Consider first an initial arrangement of N domains on a ring. There are $N!$ ways for this system to coarsen, i.e., N possibilities for the first domain to disappear, $N-1$ possibilities for the second, etc. Each possibility is weighted with a probability that is a function of the rates of disappearance of the N domains. Summing over the $(N-1)!$ possible initial arrangements of the N domains on the ring implies $N!(N-1)!$ possible ''histories'' for the dynamics.

Now note that if the domains are uncorrelated then the dynamics becomes equivalent to a mean-field model (often referred to as a bag model or an independent intervals theory): when a domain is eliminated one picks a domain at random to be its right neighbor and coalesces the two. In this dynamics there are at each step $N(N-1)$ possibilities: the factor N comes from which domain is eliminated and the factor $N-1$ from which domain is picked to be its neighbor. Therefore for N initial domains there are $N!(N-1)!$ possible histories, each weighted by the probability for the domains to be eliminated in the specified sequence. These possible histories are in one-to-one correspondence with the possible histories for the full model when summed over all possible initial arrangements. One also easily verifies that the probabilities with which these histories occur, as well as the distributions for the times that separate successive events within each history, are the same in both cases. This proves that throughout the irreversible coarsening process the domains are uncorrelated.

B. Energy barriers

We now estimate the typical time scale $\Gamma^{-1}(d)$ for the disappearance of domains of length d through coalescence with their right neighbors. This then defines a typical rate $\Gamma(d)$ for the elimination of domains. Because domain coalescence corresponds to the flipping down of up-spins, $\Gamma(d)$ can also be defined as follows. Consider an open spin chain of length d, with a ''clamped'' up-spin ($s_0=1$) added on the left. Starting from the state $(s_0,s_1,\ldots,s_d)=10\ldots01$, $\Gamma^{-1}(d)$ is the typical time needed to reach the ''empty'' state $10\ldots00$ where spin s_d has relaxed, i.e., has flipped down. Any instance of this relaxation process can be thought of as a path connecting the two states. Let us call the maximum number of ''excited'' spins (up-spins except s_0) encountered along a path its height h. One might think that the relaxation of spin s_d needs to proceed via the state $11\ldots1$, giving a path of height d. In fact, the minimal path height $h(d)$ is much lower and is given by

$$h(d)=n+1 \text{ for } 2^{n-1}<d\leqslant 2^n, \tag{11}$$

where $n=0,1,\ldots$.

To get a feel for the result (11) consider in Fig. 1 some small domain sizes. The figure illustrates that to generate an up-spin adjacent to that to be relaxed (which is the first spin of the next domain on the right) one can proceed via a sequence of stepping stones, e.g., for $d=4$ one first generates an isolated up-spin in the middle of the domain, then uses this stepping stone to generate the subsequent excited spins in a similar manner to the relaxation of a $d=2$ domain. Iteration of this argument straightforwardly proves Eq. (11) for $d=2^n$ [35].

$d=1$ $1\underline{1}\rightarrow 10$ $h(1)=1$

$d=2$ $101\rightarrow 1\underline{11}\rightarrow 110\rightarrow 100$ $h(2)=2$

$d=3$ $1001\rightarrow 1101\rightarrow 1\underline{111}\rightarrow$

$\cdots\rightarrow 1000$ $h(3)=3$

$d=4$ $10001\rightarrow\cdots\rightarrow 1\underline{11}0\underline{1}\rightarrow$

$10101\rightarrow 10\underline{111}\rightarrow\cdots\rightarrow$

$10100\rightarrow\cdots\rightarrow 10000$ $h(4)=3$

FIG. 1. Elimination of a domain of size d. Shown are paths through spin configurations that traverse the minimum energy barrier. The height of the barrier is $h(d)$ and the excited spins are underlined in the highest energy configuration(s) along the path.

In order to prove Eq. (11) generally we introduce the quantity $l(h,k)$ which is defined for the open chain discussed above. It is the length of the longest configuration that contains exactly k up-spins, always counted ignoring the fixed up-spin s_0, and that can be reached from an initially empty chain (again, except for s_0) along some path of height h. The length of a configuration is defined here as the position of the furthest up-spin to the right. Note that $l(h,k)>l(h,k-1)$; thus $l(h,h)$ gives the longest configuration that can be reached along any path of height h.

Now consider how a configuration realizing $l(h,k)$ could be constructed. First one generates an isolated up-spin as far to the right as possible. This distance is $l(h,1)$. Then one starts from the up-spin just generated to generate a second up-spin as far to the right of the first as possible. Since the first up-spin remains up, there is one less unit of energy to play with to generate the second up-spin and the total distance from the origin will be $l(h,1)+l(h-1,1)$. Continuing in this fashion to generate all k up-spins, one arrives at

$$l(h,k)=\sum_{m=1}^{k} l(h-m+1,1). \tag{12}$$

To close the set of equations (12) we need an expression for $l(h,1)$. This can be obtained by invoking the reversibility of paths: since the dynamics obeys detailed balance, the existence of a path of height h from an initial to a final state implies that the reversed path connects the final to the initial state and is also of height h. Thus $l(h,1)$ gives the size of the longest domain that can be relaxed along some path of height h. It is easy to see that the final step in this process requires an up-spin adjacent to the up-spin that is to be relaxed. Since, with this latter up-spin, we have already used up one unit of energy or height, the maximum distance from the origin at which such an up-spin could be generated is $l(h-1,h-1)$. Therefore we conclude

$$l(h,1)=l(h-1,h-1)+1 \tag{13}$$

with boundary condition $l(0,0)=0$. Inserting Eq. (13) into Eq. (12) gives

$$l(h,k)=\sum_{m=1}^{k} l(h-m,h-m)+k. \tag{14}$$

Setting $k=h$, Eq. (14) has solution $l(h,h)=2^h-1$. Substituting this back into Eq. (14) yields

$$l(h,k)=2^h-2^{h-k}. \tag{15}$$

In particular the longest domain that can be relaxed via a path of height $h=n+1$ is given by $l(n+1,1)=l(n,n)+1=2^n$ from which we deduce Eq. (11). Related results on the number of configurations reachable at or below height h can be found in Ref. [36].

C. Solution of the dynamics

From result (11) it follows that the coarsening dynamics naturally divides into stages distinguished by $n=h(d)-1=0,1,\ldots$. During stage n, the domains with lengths $2^{n-1}<d\leqslant 2^n$ disappear; we call these the "active" domains. This process takes place on a time scale of $O(\Gamma^{-1}(d))=O(\epsilon^{-n})$; because the time scales for different stages differ by factors of $1/\epsilon$, we can treat them separately in the limit $\epsilon\rightarrow 0$. Thus during stage n active domains are eliminated. The distribution of inactive domains ($d>2^n$) changes because elimination of an active domain implies coalescence with a neighboring domain on the right; since the smallest active domains have length $d=2^{n-1}+1$, any new domain will have length $\geqslant 2(2^{n-1}+1)>2^n$ and thus be inactive.

Let $N(d,t)$ be the number of domains of length d at time t, $N(t)=\Sigma_d N(d,t)$ be the total number of domains, and $P(d,t)=N(d,t)/N(t)$ be the domain size distribution. Then for a general process of coarsening by coalescence one has, using that there are no spatial correlations between domains,

$$\frac{\partial}{\partial t}N(d,t)=-\Gamma(d)N(d,t)-N(d,t)\sum_{d'}\Gamma(d')P(d',t)+\sum_{d'}N(d-d',t)\Gamma(d')P(d',t). \tag{16}$$

The first term accounts for the disappearance of a domain by coalescence with its right neighbor, the second for coalescence with a domain on the left of length d', and the third for creation of larger domains during coalescence. Summing Eq. (16) over d one finds $\partial N(t)/\partial t=-\Sigma_d\Gamma(d)N(d,t)$, and hence

$$\frac{\partial}{\partial t}P(d,t)=-\Gamma(d)P(d,t)+\sum_{d'}P(d-d',t)\Gamma(d')P(d',t). \tag{17}$$

We now apply this general result to the scenario at hand. We change to a rescaled time variable appropriate to the nth stage of the dynamics, $\tau=t\epsilon^n$. To be in the nth stage, t has to obey the restrictions $\epsilon^{-(n-1)}\ll t\ll\epsilon^{-(n+1)}$, giving $\epsilon\ll\tau\ll\epsilon^{-1}$; in the limit $\epsilon\rightarrow 0$ we can thus let τ range over $[0,\infty]$. The rescaled rates $\tilde{\Gamma}(d)=\epsilon^{-n}\Gamma(d)$ are nonzero only for the domains with $d\leqslant 2^n$; on the other hand, $P(d,\tau)$ is nonzero

only for $d>2^{n-1}$ since smaller domains have disappeared during earlier stages. Thus the sum over d' on the right-hand side (rhs) of Eq. (17) is restricted to $2^{n-1}<d'\leqslant 2^n$, i.e., the active domains. Furthermore, if d is an active domain then $d-d'<2^{n-1}$ and hence the factor $P(d-d',t)$ vanishes for every term in the sum, reflecting the fact that active domains cannot be created. Equation (17) thus becomes for $2^{n-1}<d\leqslant 2^n$

$$\frac{\partial}{\partial\tau}P(d,\tau)=-\tilde{\Gamma}(d)P(d,\tau). \tag{18}$$

For $d>2^n$, on the other hand, the *first* term in Eq. (17) does not contribute and one gets

$$\frac{\partial}{\partial\tau}P(d,\tau)=\sum_{2^{n-1}<d'\leqslant 2^n}P(d-d',t)\tilde{\Gamma}(d')P(d',t). \tag{19}$$

Combining the last two results one finds that the rates drop out, giving for $d>2^n$

$$\frac{\partial}{\partial\tau}P(d,\tau)=\sum_{2^{n-1}<d'\leqslant 2^n}P(d-d',\tau)\left[-\frac{\partial}{\partial\tau}P(d',\tau)\right]. \tag{20}$$

There is one subtlety in this derivation which we have so far ignored. Even in terms of the rescaled time τ, i.e., taking into account only those relaxation processes that cross the minimum energy barrier of n, the ''survival probability'' for a domain not to have coalesced with its right neighbor is not necessarily a single exponential which can be characterized by a rate constant $\tilde{\Gamma}(d)$ [37]. This is because several relaxation processes with different rescaled rates of $O(1)$ may exist. In Eqs. (18) and (19) one should then replace $\tilde{\Gamma}(d)$ by the negative derivative of the survival probability, resulting in an effective, time-dependent rate $\tilde{\Gamma}(d,\tau)=-[\partial P(d,\tau)/\partial\tau]/P(d,\tau)$; but the rates can again be eliminated and Eq. (20) follows as before. Note that equation (20) in fact also has a simple intuitive meaning: it expresses the fact that active domains eliminated during the nth stage coalesce with neighboring domains of random size, forming stable domains of size $d>2^n$. Equation (20) then determines the time dependence of the size distribution of the inactive domains for a given time dependence of the distribution of the active domains.

To solve the equation of motion (20) we define the generating function

$$G(z,\tau)=\sum_{d=2^{n-1}+1}^{\infty}P(d,\tau)z^d \tag{21}$$

and its analog for the active domains,

$$H(z,\tau)=\sum_{d=2^{n-1}+1}^{2^n}P(d,\tau)z^d. \tag{22}$$

Then multiplying Eq. (20) by z^d and summing over $d>2^n$ yields

$$\begin{aligned}\frac{\partial}{\partial\tau}&[G(z,\tau)-H(z,\tau)]\\&=\sum_{d=2^n+1}^{\infty}\sum_{d'=2^{n-1}+1}^{2^n}P(d-d',\tau)\left[-\frac{\partial}{\partial\tau}P(d',\tau)\right]z^d\\&=\sum_{d''=2^{n-1}+1}^{\infty}\sum_{d'=2^{n-1}+1}^{2^n}P(d'',\tau)\left[-\frac{\partial}{\partial\tau}P(d',\tau)\right]z^{d''+d'}\\&=-G(z,\tau)\frac{\partial}{\partial\tau}H(z,\tau),\end{aligned} \tag{23}$$

where we have used that in stage n of the dynamics $P(d'',\tau)=0$ for $d''\leqslant 2^{n-1}$. We may integrate Eq. (23) by rewriting it as

$$\frac{1}{[1-G(z,\tau)]}\frac{\partial}{\partial\tau}G(z,\tau)=\frac{\partial}{\partial\tau}H(d,\tau) \tag{24}$$

giving

$$\frac{1-G(z,\tau)}{1-G(z,0)}=\exp[-H(z,\tau)+H(z,0)]. \tag{25}$$

At the end of stage n, corresponding to $\tau\to\infty$, all domains that were active during that stage have disappeared, and so $H(z,\infty)=0$. Thus

$$G(z,\infty)-1=[G(z,0)-1]\exp[H(z,0)]. \tag{26}$$

Now recall that we are considering stage n of the dynamics. The initial condition for stage $n+1$ of the dynamics will be given by the distribution $P(d,t)$ at the end of stage n. Thus defining $G_n(z)\equiv G(z,0)$ for stage n, with a similar definition for the active generating function $H_n(z)$, Eq. (26) relates the different stages of the dynamics through

$$G_{n+1}(z)-1=[G_n(z)-1]\exp[H_n(z)]. \tag{27}$$

This exact result connects, through their generating functions, $P_n(d)$ and $P_{n+1}(d)$ which are defined as the domain length distributions at the end of stages $n-1$ and n of the dynamics, respectively. It can be checked that for $n=0$, where the system does not cross energy barriers, Eq. (27) gives results compatible with the known exact solution of the $T=0$ dynamics [22].

Iterating Eq. (27) from a given initial distribution $P_0(d)$ gives $P_n(d)$ for all $n=1,2,\ldots$. Figure 2 shows numerical results for the case where $P_0(d)$ is the equilibrium distribution (8) corresponding to an initial temperature of $T=\infty$. It is clear that a scaling limit emerges for large n, i.e., that the rescaled distributions

$$\tilde{P}_n(x)=2^{n-1}P_n(d)\quad\text{where } x=\frac{d}{2^{n-1}} \tag{28}$$

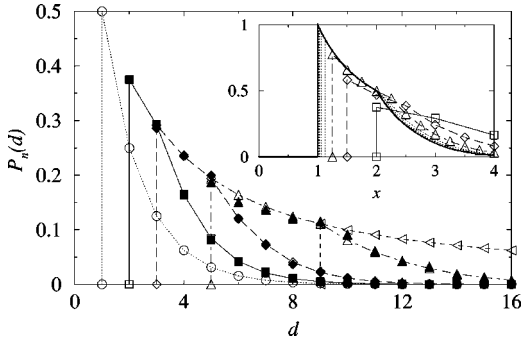

FIG. 2. Domain length distributions $P_n(d)$ at the end of stage $n-1$ of the low-T coarsening dynamics, for initial temperature $T=\infty$. Open symbols and lines: theoretical results, calculated from Eq. (27), for $n=0$ (○; initial condition), 1 (□), 2 (◇), 3 (△). Filled symbols: simulation results for a chain of length $L=2^{15}$ and $\epsilon=10^{-4}$ ($n=1,2$) and $\epsilon=10^{-3}$ ($n=3$). Inset: Scaled predictions $2^{n-1}P_n(d=2^{n-1}x)$ vs x for $n=1,\ldots,8$. Thick line: predicted scaling function (31).

converge to a limiting distribution $\tilde{P}(x)$ for the scaled domain size x. This is just a statement of the invariance of the coarsening processes in each stage once the domain sizes are rescaled by the characteristic size 2^{n-1}.

The change to a continuous variable x for the domain lengths simply results in the generating functions $G_n(z), H_n(z)$ being replaced by Laplace transforms $g_n(s)$ and $h_n(s)$, via the correspondence $z^d \to e^{-sx}$. Invariance of the scaled domain distribution under Eq. (27) then gives the equation

$$g(2s)-1=[g(s)-1]\exp[h(s)], \tag{29}$$

where

$$g(s)=\int_1^\infty dx\tilde{P}(x)e^{-sx}, \quad h(s)=\int_1^2 dx\tilde{P}(x)e^{-sx}.$$

We found a solution to Eq. (29) by noting that the numerics strongly suggest $\tilde{P}(x)=1/x$ for $1<x<2$. Using this as an ansatz implies

$$h(s)=\mathrm{Ei}(s)-\mathrm{Ei}(2s) \quad \text{where} \quad \mathrm{Ei}(s)=\int_s^\infty \frac{e^{-u}}{u}du,$$

which when inserted into Eq. (29) yields

$$[1-g(s)]\exp[\mathrm{Ei}(s)]=\text{const.}$$

The requirement that $g(s)\to 0$ for large s fixes the constant as unity, giving

$$g(s)=1-\exp[-\mathrm{Ei}(s)]. \tag{30}$$

Expanding the exponential as a series allows the Laplace transform to be inverted term by term and one obtains

$$\begin{aligned}\tilde{P}(x)&=\frac{1}{2\pi i}\int_{\gamma-i\infty}^{\gamma+i\infty}dse^{sx}g(s)\\&=\frac{1}{2\pi i}\int_{\gamma-i\infty}^{\gamma+i\infty}dse^{sx}\sum_{m=1}^{\infty}\frac{(-1)^{m+1}}{m!}\mathrm{Ei}^m(s)\\&=\sum_{m=1}^{\infty}\frac{(-1)^{m+1}}{m!}\int_1^\infty\prod_{j=1}^{m}\frac{du_j}{u_j}\delta\left(\sum_{k=1}^{m}u_k-x\right)\\&=\Theta(x-1)\frac{1}{x}-\Theta(x-2)\frac{\ln(x-1)}{x}+\ldots,\end{aligned} \tag{31}$$

where $\Theta(x)$ is the Heaviside step function. This result for the scaling function is shown in Fig. 2 and shows good agreement with the numerically calculated $P_n(d)$ for large n. Note that series (31) has singularities in the kth derivative at the integer values $x=k+1,\ k+2,\ldots,$ a fact whose physical origin we discuss further in the following. The average domain length in the scaling limit is given by $\overline{d_n}=2^{n-1}\overline{x}$; from the results for $\tilde{P}(x)$ we find $\overline{x}=\exp(\gamma)=1.78\ldots$, where γ is Euler's constant.

D. A family of related coarsening models

Surprisingly, the scaling function (31) for coarsening dynamics in the East model is identical to that for the ''paste-all'' model of coarsening dynamics, where at each step in the dynamics the shortest domain is selected and ''pasted'' onto its left or right neighbor [31]. To understand this, we decide for definiteness that domains are to be pasted to the right. Then the paste-all model can be obtained from a modification of the hierarchical coarsening dynamics discussed so far—one merely needs to assume that the rates $\Gamma(d)$ are now *all* well separated from each other, so that at any given stage in the dynamics only domains of a single size d are active. It is then natural to consider a family of models which interpolates between the paste-all and the East model, by assuming that the active domain sizes d at any stage n—whose coalescence rates $\Gamma(d)$ are comparable to each other but well separated from all other rates—are those with $a^{n-1}<d\leq a^n$, with a a constant in the range $1<a\leq 2$.

All of the arguments in the preceding section apply to this modified model if powers of 2 are replaced by powers of a in the appropriate places. In particular, Eq. (29) for the Laplace transform of the scaling distribution becomes

$$g(as)-1=[g(s)-1]\exp[h_a(s)] \tag{32}$$

with

$$h_a(s)=\int_1^a dx\tilde{P}(x)e^{-sx} \tag{33}$$

generalizing the earlier $h(s)\equiv h_2(s)$. We now show that Eq. (32) has the same family of solutions for any $a\leq 2$, thus proving in particular the link between the scaling distributions of the East model ($a=2$) and the paste-all model ($a\to 1$). To see this, consider first $a\to 1$; we should then re-

cover the scaling equation for the paste-all model. Indeed, setting $a=1+\delta$ and expanding to first order in δ, Eq. (32) becomes

$$sg'(s)=[g(s)-1]\tilde{P}(1)e^{-s}, \tag{34}$$

which is equivalent to Eq. (38) in Ref. [31]. Integrating Eq. (34) gives [31] $g(s)=1-\exp[-\tilde{P}(1)\mathrm{Ei}(s)]$, and the Laplace transform can be inverted as in Eq. (31), giving

$$\tilde{P}(x)=\Theta(x-1)\frac{\tilde{P}(1)}{x}-\Theta(x-2)\frac{\tilde{P}^2(1)\ln(x-1)}{x}+\cdots.$$

Given that only the first term contributes for $x\leqslant 2$, it is now easy to verify that this is also a solution of Eq. (32) for any $a\leqslant 2$: from Eq. (33) one has $h_a(s)=-\tilde{P}(1)[\mathrm{Ei}(as)-\mathrm{Ei}(s)]=\ln[1-g(as)]-\ln[1-g(s)]$.

In summary, we have shown that there is a whole family of coarsening models that interpolate between the paste-all and East models and which have the same scaling solution. The solution is, in principle, parametrized by $\tilde{P}(1)$ but, as discussed in Ref. [31], the requirement of a finite mean for the scaling distribution imposes $\tilde{P}(1)=1$. Thus $g(s)=1-\exp[-\mathrm{Ei}(s)]$ as we found in Eq. (30).

Physically, the common feature of all the models in the family is that active domains can never be created during the stage where they are active; this breaks down for $a>2$ where indeed the scaling solution no longer applies. This argument clarifies the origin of the singularities at integer arguments of $\tilde{P}(x)$: the existence of a shortest scaled domain length $x=1$ implies that the shortest inactive domain that can be created has $x=2$, and this effect then propagates to $x=3,4,\ldots$, as the dynamics is iterated. We initially thought the fact that in the East model the active domains cover a range $x\in[1,2]$ bounded by two integers, was significant. However, this is clearly not the case since for general $a\leqslant 2$ this range becomes $x\in[1,a]$.

E. Anomalous coarsening

Having solved the dynamics in terms of the different stages labeled by n, we now translate these results into actual time dependencies. As before, we consider a system quenched from, say, $T=\infty$, to a temperature $T\ll 1$ at time $t=0$. If data for, e.g., the average domain length $\overline{d}$ are plotted against the scaled time variable $\nu=T\ln t$, then for $T\to 0$ the nth stage of the dynamics shrinks to the point $\nu=n$. In this limit we predict that, for $n-1<\nu<n$, the domain length distribution is $P_n(d)$ as defined by recursion (27). The average domain length $\overline{d}(\nu)$ will follow a "staircase" function, jumping at $\nu=n$ from $\overline{d}_n=\Sigma_d P_n(d)d$ to $\overline{d}_{n+1}$. This was illustrated and verified by low-T simulations in Ref. [17].

For large n, i.e., in the scaling regime of large $\overline{d}$ (but still $\overline{d}\ll\overline{d}_{\mathrm{eq}}$), we know that $\overline{d}_n=2^{n-1}\overline{x}$ where $\overline{x}=1.78\ldots$. The staircase function $\overline{d}(\nu)$ is therefore bounded between $2^{\nu-1}\overline{x}\leqslant\overline{d}\leqslant 2^{\nu}\overline{x}$, giving $\frac{1}{2}\leqslant\overline{d}/(\overline{x}t^{T\ln 2})\leqslant 1$ when expressed in terms of ordinary time t. This shows that the hierarchical dynamics gives rise to anomalous coarsening, i.e., the typical domain size grows as $\overline{d}\sim t^{T\ln 2}$, more slowly in time than a usual power law with T-independent exponent. The exponent can also be deduced from the scaling $t\sim\Gamma(\overline{d})^{-1}\sim\epsilon^n=\exp(n/T)$ of the time required to eliminate a domain of the typical size $\overline{d}$. Since $\overline{d}\sim 2^n$ asymptotically, one has $n\approx\ln\overline{d}/\ln 2$ and this time scales as $t\sim\overline{d}^{1/T\ln 2}$, giving $\overline{d}\sim t^{T\ln 2}$ as before. For decreasing T the coarsening becomes anomalously slow and in fact logarithmic for $T\to 0$.

By extrapolating the anomalous coarsening law to the equilibrium domain length $\overline{d}_{\mathrm{eq}}=\exp(1/T)+O(1)$, we can estimate the equilibration time of the system for $T\to 0$ as $t_{\mathrm{eq}}\sim t_*=\exp(1/T^2\ln 2)$. Of course, in performing this extrapolation, we are using the anomalous coarsening law in the regime where domain sizes are $O(1/\epsilon)$ and the assumption of irreversible down-flips no longer holds. Given this we could have equally well extrapolated $\overline{d}\sim t^{T\ln 2}$ to some multiple $\alpha\overline{d}_{\mathrm{eq}}$ of the equilibrium domain length, which would yield $t_{\mathrm{eq}}=\exp(1/T^2\ln 2-A/T)$ with $A=-\ln\alpha/\ln 2$. With the sign as defined, A should be positive, corresponding to $\alpha<1$; a negative value of A is excluded as it would violate the relaxation time bound of Ref. [12]. Thus we expect t_* to give only the dominant divergence of the equilibration time t_{eq}, with subdominant correction factors $\exp(-A/T)$ making $t_{\mathrm{eq}}\ll t_*$ generically. Our analysis in Sec. IV suggests, on the other hand, that the longest relaxation time scales *at* equilibrium are given directly by t_*. This is not unreasonable: the time to reach equilibrium from an initial high-temperature configuration is expected to be much shorter than the time for correlations to be erased starting from an equilibrium (low-temperature) initial condition, simply because the typical domains to be eliminated are shorter.

Finally, we comment briefly on the implications of the coarsening dynamics for the two-time spin autocorrelation function $C(t,t_{\mathrm{w}})=\langle s_i(t)s_i(t_{\mathrm{w}})\rangle-\langle s_i(t)\rangle\langle s_i(t_{\mathrm{w}})\rangle$, where $t>t_{\mathrm{w}}$. Since in the limit $T\to 0$ spins flip down irreversibly, $s_i(t)=1$ implies that $s_i(t_{\mathrm{w}})=1$ at the earlier time t_{w}, thus $C(t,t_{\mathrm{w}})=c(t)[1-c(t_{\mathrm{w}})]$ where $c(t)$ is the time-dependent up-spin concentration. As a function of t, $C(t,t_{\mathrm{w}})$ will thus exhibit the same plateaux as $c(t)$, and these were indeed observed in the simulations of Ref. [22]. Also, the normalized autocorrelation becomes simply $C(t,t_{\mathrm{w}})/C(t_{\mathrm{w}},t_{\mathrm{w}})=c(t)/c(t_{\mathrm{w}})=\overline{d}(t_{\mathrm{w}})/\overline{d}(t)$. This dependence on only the ratio of the relevant length scales at times t_{w} and t is natural for a coarsening process, and gives a good fit to the data of Ref. [22].

IV. EQUILIBRIUM DYNAMICS

A. Functions of interest

We now turn to the equilibrium dynamics of the East model at low temperatures. These are encoded in relaxation functions such as correlations and spin persistence (see below); response functions provide no new information since they are related to correlations via the fluctuation-dissipation theorem (FDT). For correlation functions standard choices would be the local spin autocorrelation $\langle s_i(t)s_i(0)\rangle-c^2$ or

the correlation function of the up-spin concentration (or magnetization) $M(t)=(1/L)\Sigma_i s_i(t)$. However, the directionality of the kinetic constraint can be shown to imply that all nonlocal correlations $\langle s_i(t)s_j(0)\rangle - c^2$ vanish [38] so these two choices give the same information. We can thus focus on the normalized autocorrelation function

$$C(t)=\frac{\langle s_i(t)s_i(0)\rangle - c^2}{c-c^2}=\frac{P(s_i(t)=1|s_i(0)=1)-c}{1-c}. \tag{35}$$

This decays from $C(0)=1$ to $C(t\to\infty)=0$; the second equality in Eq. (35) implies that it is essentially the conditional probability for an up-spin that was up at time 0 also to be up at time t. Closely related is the up-spin persistence function $\mathcal{P}_1(t)$, which gives the probability that a spin is up throughout the time interval $[0,t]$, and the analogously defined down-spin persistence $\mathcal{P}_0(t)$.

Fortunately, it turns out that C, $\mathcal{P}_1$, and $\mathcal{P}_0$ do not need to be analyzed separately because they all become identical in the limit $T\to 0$ [taken at a constant value of, say, $C(t)$] that we are interested in. To see this, note that since in the East model the spins are only coupled via the kinetic constraint, which acts to the right, the dynamics of a spin s_i cannot influence that of its left neighbor s_{i-1}. (This is strictly true only in the limit of an infinite chain $L\to\infty$, but that is precisely the case of interest.) Furthermore, the dynamical evolution of spin s_i is that of a single spin in a field whenever $s_{i-1}=1$, and is completely frozen otherwise. It follows that if, between times 0 and t, s_{i-1} has been up a fraction m of the time, then the evolution of s_i has been that of a single spin over time mt. But the single-spin correlation and persistence functions are trivial to work out; denoting the distribution of m for a given t by $P(m;t)$, one thus has the simple expressions

$$C(t)=\int_0^1 dm P(m;t)e^{-(1+\epsilon)mt}, \tag{36}$$

$$\mathcal{P}_1(t)=\int_0^1 dm P(m;t)e^{-mt}, \tag{37}$$

$$\mathcal{P}_0(t)=\int_0^1 dm\, P(m;t)e^{-\epsilon mt}. \tag{38}$$

It follows trivially that

$$C(t)\leqslant\mathcal{P}_1(t)\leqslant\mathcal{P}_0(t). \tag{39}$$

Now since $P(s_i(t)=1|s_i(0)=1)\geqslant\mathcal{P}_1(t)$ (the probability for a spin to be up at times 0 and t must be greater than that for it to be up at 0 and t *and* all intermediate times), one has from Eq. (35)

$$(1-c)C(t)+c\geqslant\mathcal{P}_1(t). \tag{40}$$

Equations (39) and (40) together show that $C(t)$ and $\mathcal{P}_1(t)$ coincide in the low-T limit ($c\approx\epsilon\to 0$) whenever the values of the functions themselves are of $O(1)$.

To get the analogous result for C and $\mathcal{P}_0$, consider $P(m;t)$. The concentration of persistent up-spins and down-spins in the system is $c\mathcal{P}_1(t)$ and $(1-c)\mathcal{P}_0(t)$, respectively, and these have $m=1$ and $m=0$. Thus

$$P(m;t)=(1-c)\mathcal{P}_0(t)\,\delta(m)+c\mathcal{P}_1(t)\,\delta(m-1)+\cdots, \tag{41}$$

where the dots indicate contributions for m strictly between 0 and 1. Inserting into Eq. (37) and separating off the $\delta(m)$ term gives

$$\mathcal{P}_1(t)=(1-c)\mathcal{P}_0(t)+\int_{>0}^1 dm P(m;t)e^{-mt}\geqslant(1-c)\mathcal{P}_0(t).$$

Together with Eq. (39) it follows that also $\mathcal{P}_1(t)$ and $\mathcal{P}_0(t)$ coincide for $c\to 0$. Thus $C=\mathcal{P}_1=\mathcal{P}_0$ in the limit, and we can restrict attention to, e.g., the up-spin persistence $\mathcal{P}_1(t)$ in the following.

We stress once more that the directionality of the kinetic constraint is essential for the above arguments to work. In the undirected version of the East model, i.e., the one-dimensional Fredrickson-Andersen model with $f=1$, it would still be true that the dynamics of spin s_i is determined by the amount of time that s_{i-1} (and s_{i+1}) spend in the up-state. But this time cannot be determined independently of the state of spin s_i, since s_i itself affects the dynamics of s_{i-1} (and s_{i+1}).

B. First passage times

To get some insight into the equilibrium dynamics, we generalize the domain coalescence rates $\Gamma(d)$, discussed in Sec. III for $d=O(1)$ and $\epsilon\to 0$, to the regime of domain sizes typically found in equilibrium, $d\sim\overline{d}_{\rm eq}\approx 1/\epsilon$. Starting from the state $(s_0,s_1,\ldots,s_d)=10\ldots01$, we define a mean first passage time (MFPT) $\tau_{\rm mfp}(d)$ as the mean time for the spin s_d to flip down for the first time, and we set $\Gamma(d)=\tau_{\rm mfp}^{-1}(d)$. Note that in Sec. III B we required for a "first passage" that not just s_d but all other spins $s_1,\ldots,s_{d-1}$ be down; here we just require that $s_d=0$. In the regime considered in Sec. III, the two definitions are equivalent to leading order, since the relaxation process has passed its "highest point" once s_d has flipped down, resulting in the same energy barrier whether or not the process continues to the empty state.

Consider now the dependence of $\tau_{\rm mfp}(d)$ on d. From the discussion of the out-of-equilibrium dynamics we know that $\tau_{\rm mfp}(d)$ exhibits a steplike variation with d for $d=O(1)$ and small ϵ, varying only by factors of order unity within each range $2^{n-1}<d\leqslant 2^n$ but increasing by $\sim\epsilon^{-1}$ between ranges. As n increases at fixed ϵ, however, the $O(1)$ changes within ranges become larger and eventually comparable to ϵ^{-1}; $\tau_{\rm mfp}(d)$ will then increase more smoothly with d. The numerically simulated MFPTs in Fig. 3 confirm this. Finally, for d larger than $\overline{d}_{\rm eq}\approx 1/\epsilon$, the figure shows that the MFPTs increase linearly with d. Intuitively, one then has a "front" of up-spins that creeps "ballistically" along the chain. This can be motivated by arguing that, for d above the typical equi-

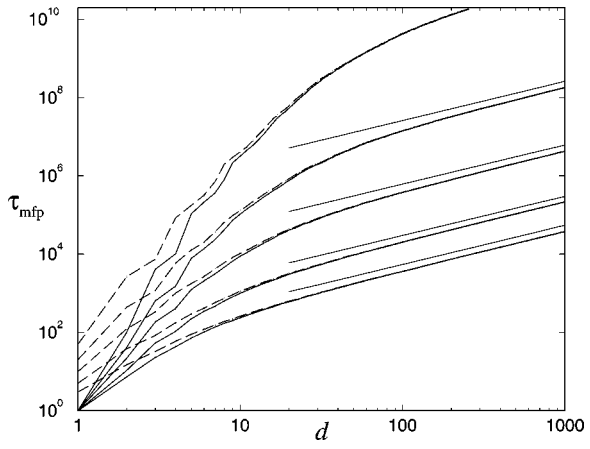

FIG. 3. Simulated MFTPs $\tau_{\rm mfp}$ for down-flips (solid) and $\tau'_{\rm mfp}$ for up-flips (dashed) as a function of unscaled distance d, for $\epsilon = 0.3,0.2,0.1,0.05,0.02$ (bottom to top). The thin solid lines have slope 1, showing that for large d the MFPTs vary linearly with d. Error bars are too small to show on the scale of the plot ($\leqslant 3.5\%$ relative error on $\tau_{\rm mfp}$ and $\tau'_{\rm mfp}$).

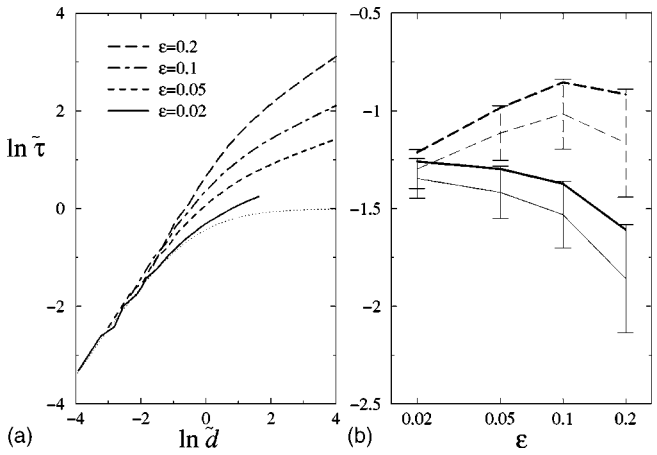

FIG. 4. (a) Logarithmic plot of scaled FPTs $\tilde{\tau}$, as defined in Eq. (42), vs scaled distance $\tilde{d}$, for $\epsilon = 0.2,0.1,0.05,0.02$ (top to bottom on right). The dotted line shows a qualitative sketch of the scaling function $f(\tilde{d})$, with $f\to 1$ ($\ln f\to 0$) for $\tilde{d}\to\infty$; see text. (b) Up-flip (dashed) vs down-flip (solid) FPTs and their fluctuations vs ϵ for constant $\tilde{d} = \epsilon d = 0.1$. Thin lines and error bars: mean and $\pm\frac{1}{2}$(standard deviation) of the log-rescaled FPT $\ln\tilde{\tau}$. Thick lines: $\ln\tilde{\tau}_{\rm mfp}$. As ϵ decreases, the fluctuations in $\ln\tilde{\tau}$ are seen to decrease: error bars shrink, and $\ln\tilde{\tau}_{\rm mfp}$ and the mean of $\ln\tilde{\tau}$ become closer. Also, up-flip and down-flip times become closer; both observations support our scaling hypothesis for the FPTs.

librium length scale $\overline{d}_{\rm eq}$, the spin front no longer remembers that it originated from a single up-spin a distance d to the left. Instead it behaves as on an infinite chain, where its propagation velocity is necessarily constant.

So far we have considered the variation of $\tau_{\rm mfp}(d)$ with d at fixed ϵ. One suspects, however, that, e.g., the decay of the persistence function $\mathcal{P}_1(t)$ is governed by a length scale $d(t)$, giving the size of the largest domains that have had time to equilibrate, and more precisely—since we are considering equilibrium dynamics—by the ratio $d(t)/\overline{d}_{\rm eq}$. We thus define scaled domain sizes $\tilde{d} = \epsilon d$ ($= d/\overline{d}_{\rm eq}$ for $\epsilon\to 0$) and now ask how $\tau_{\rm mfp}(\tilde{d})$ scales with T for *fixed* $\tilde{d}$. For small $\tilde{d}$, extrapolating from the regime of $d = O(1)$, and using $n \approx \ln d/\ln 2$, one expects

$$\tau_{\rm mfp}(\tilde{d}) \sim \epsilon^{-\ln d/\ln 2} = \epsilon^{-\ln\tilde{d}/\ln 2 - 1/(T\ln 2)}$$
$$= \exp\left(\frac{\ln\tilde{d}}{T\ln 2} + \frac{1}{T^2\ln 2}\right).$$

Rearranging, one has

$$\left(\frac{\tau_{\rm mfp}(\tilde{d})}{t_*}\right)^{T\ln 2} \sim \tilde{d}.$$

From the downward curvature of the lines in Fig. 3, one sees that this expression will not be valid for larger $\tilde{d}$, where the rhs will cross over to a slower increase with $\tilde{d}$. We thus make a *time scaling hypothesis* which replaces $\tilde{d}$ by a more general scaling function $f(\tilde{d})$ of $\tilde{d}$, i.e., we assume that the rescaled MFPT approaches

$$\tilde{\tau}_{\rm mfp}(\tilde{d}) \equiv \left(\frac{\tau_{\rm mfp}(\tilde{d})}{t_*}\right)^{T\ln 2} \to f(\tilde{d}) \quad \text{for} \quad T\to 0 \qquad (42)$$

when the limit is taken at fixed $\tilde{d}$. Figure 4(a) represents numerical data for the MFPTs in this scaled form and shows that the assumption (42) is certainly plausible for not-too-large $\tilde{d}$. For larger $\tilde{d}$, convergence to a scaling limit is not yet evident from the data that we can generate on practical simulation time scales. This is because for $d \gg \overline{d}_{\rm eq}$ the ballistic propagation discussed above implies $\tilde{\tau}_{\rm mfp} \propto d^{T\ln 2} \propto \tilde{d}^{T\ln 2}$ which will tend to a constant as $T\to 0$ but does so very slowly. For the scaling function $f(\tilde{d})$ this implies that it must approach a constant as $\tilde{d}\to\infty$; recall that this limit is taken *after* the limit $T\to 0$ at fixed $\tilde{d}$. We note that the bounds of Ref. [12] imply that the MFPTs $\tau_{\rm mfp}$ cannot exceed t_* by more than factors of $O(1)$; this implies from Eq. (42) that $f(\tilde{d}) \leqslant 1$. Our numerical data in Fig. 4(a) are restricted to values of T which are still too large to determine $f(\tilde{d})$ with any accuracy, but the tentative extrapolation to $T\to 0$ indicated in the figure is certainly consistent with the bound $f(\tilde{d}) \leqslant 1$.

We work below with a slightly strengthened version of Eq. (42). The first passage time τ for down-flips is a fluctuating quantity, with mean $\tau_{\rm mfp}$. We assume that fluctuations in τ are small enough that Eq. (42) holds even for the fluctuating τ, which means that for $T\to 0$ the rescaled FPT $\tilde{\tau}(\tilde{d}) = [\tau(\tilde{d})/t_*]^{T\ln 2}$ becomes nonfluctuating. This assumption is not as strong as it may sound; because of the exponentiation by $T\ln 2$ it holds, e.g., if the relative fluctuations of the unscaled FPT $\tau(\tilde{d})$ remain of $O(1)$ as $T\to 0$. Further confirmation comes from Fig. 4(b) which shows numerical data for $\tilde{d} = 0.1$.

In a final generalization we also assume that Eq. (42) applies if we consider FPTs τ' for *up-flips*, where we start with the empty state $10\ldots00$ and τ' is the first time where the last spin s_d has flipped up. Naively one might have suspected that τ' and τ differ by a factor $\sim 1/\epsilon$. However, the equivalence of $\mathcal{P}_1(t)$ and $\mathcal{P}_0(t)$ that we proved for low T already suggests otherwise. The correct intuition is that both up- and down-spins only become mobile once an up-spin ''front'' from an up-spin to the left has reached them, and that for $T\to 0$ the time required for this front propagation vastly dominates the effect of the different flip rates of up- and down-spins once the front has reached them. Figure 4(b) again supports this assumption with numerical data for $\tilde{d}=0.1$.

In summary, we assume in the following that Eq. (42) is valid for unaveraged up-flip and down-flip FPTs, with the same scaling function $f(\tilde{d})$. A consequence of this is *continuous time scale separation*: for any two rescaled distances $\tilde{d}_1<\tilde{d}_2$, the ratio of the corresponding FPTs is $[f(\tilde{d}_2)/f(\tilde{d}_1)]^{1/(T\ln 2)}$ and diverges as $T\to 0$. In the limit, this means that the equilibration of domains of length $\tilde{d}_1$ proceeds infinitely more quickly than for any even slightly larger length $\tilde{d}_2$. This insight is the key for the construction of the superdomain model described next. A proviso is that we have assumed here that the scaling function $f(\tilde{d})$ is strictly monotonically increasing with $\tilde{d}$. In principle, it is possible that $f(\tilde{d})$ could increase monotonically only up to some finite $\tilde{d}_*$, and be exactly constant thereafter. This seems implausible to us, however—e.g., it is difficult to conceive of a physical mechanism causing the singularity at $\tilde{d}_*$—and, as discussed below, would also give very unusual predictions for the time dependence of the low-T relaxation functions.

C. Superdomain model

We now exploit the idea of continuous time scale separation to construct an effective description for the low-T equilibrium dynamics of the East model. It is natural to work with the equilibrated length scale $\tilde{d}_\mathrm{r}$ that corresponds to the relaxation time scale t_r we are considering; from Eq. (42), the two are related by

$$\left(\frac{t_\mathrm{r}}{t_*}\right)^{T\ln 2}=f(\tilde{d}_\mathrm{r}).$$

Here and in the following, the limit $T\to 0$ (or equivalently $\epsilon\to 0$, or $c\to 0$) is always understood. For simplicity we will simply call $\tilde{d}_\mathrm{r}$ ''time'' where there is no ambiguity. We stress that we work with *rescaled* length scales $\tilde{d}=d\epsilon$ throughout; a value of $\tilde{d}$ of order unity thus corresponds to a very large domain length $d=\tilde{d}/\epsilon$ in the limit $\epsilon\to 0$.

Consider now an equilibrium configuration of the spin chain, consisting of up-spins separated by long domains of down-spins. From Eq. (8), the (rescaled) domain sizes are distributed according to a simple exponential, $P(\tilde{d})=\exp(-\tilde{d})$. A ''time'' $\tilde{d}_\mathrm{r}$ later, each of the up-spins will have developed an equilibrated zone of length $\tilde{d}_\mathrm{r}$ to its right: from continuous time scale separation, the FPT to reach any spin *within* this zone is much shorter than t_r. Throughout the zone we should thus indeed have *equilibrated* spins, which are independently up with probability $c=\epsilon/(1+\epsilon)\approx\epsilon$. The domains defined by up-spins within these equilibrated zones will not be of interest in the following. Instead we focus on the ''superdomains'' which are naturally defined by the unequilibrated up-spins, to which we refer as ''superspins.'' Thus each superdomain is bounded on the left by such a superspin, followed by an equilibrated zone of length $\tilde{d}_\mathrm{r}$ and then a string of down-spins.

To understand the dynamics of superdomains as we look at increasing times $\tilde{d}_\mathrm{r}$, it is easiest to consider a system for which the rescaled chain length ϵL and therefore the typical number of superdomains is large but finite; there is then at all times a nonzero minimum superdomain length. On increasing $\tilde{d}_\mathrm{r}$ from zero, all superspins remain as they are as long as the equilibrated zone of each superdomain has not yet reached the superspin to the right. However, when $\tilde{d}_\mathrm{r}$ becomes equal to the smallest superdomain length in the system, say $\tilde{d}_1$, then this superdomain's equilibrated zone ''catches up'' with superspin 2 bounding the next superdomain (of length $\tilde{d}_2$) on the right. This superspin now becomes equilibrated, and so one might assume that the two superdomains just coalesce, forming a single superdomain of length $\tilde{d}_1+\tilde{d}_2$. This, however, will only be the case if there are no up-spins in the equilibrated zone of superspin 2 at this time; since this zone has length $\tilde{d}_\mathrm{r}$, the probability for this event is $\exp(-\tilde{d}_\mathrm{r})$. Otherwise, i.e., with probability $1-\exp(-\tilde{d}_\mathrm{r})$, there will be at least one up-spin in the equilibrated zone of superspin 2. The leftmost of these, having lost the superspin from which it became equilibrated, becomes frozen and thus itself turns into a superspin, $2'$. The distance δ between $2'$ and the old superspin 2 has probability distribution $\exp(-\delta)/[1-\exp(-\tilde{d}_\mathrm{r})]$ over the interval $\delta\in[0,\tilde{d}_\mathrm{r}]$, and the two new superdomains have length $\tilde{d}_1'=\tilde{d}_1+\delta$ and $\tilde{d}_2'=\tilde{d}_2-\delta$ (see Fig. 5).

What makes the superdomain model nontrivial is that in the second case the process of superspin elimination and regeneration can now continue. Superspin $2'$ will immediately (on the time scale $\tilde{d}_\mathrm{r}$ being considered) equilibrate a zone of length $\tilde{d}_\mathrm{r}$. If $\tilde{d}_2'<\tilde{d}_\mathrm{r}$, then this zone includes superspin 3, which now becomes equilibrated along with a segment of length $\tilde{d}_\mathrm{r}-\tilde{d}_2'$ to its right. This, however, still leaves a segment of length $\tilde{d}_\mathrm{r}-(\tilde{d}_\mathrm{r}-\tilde{d}_2')=\tilde{d}_2'$ of the old equilibrated zone of superspin 3, which is now frozen (see Fig. 5). If there is no up-spin within this segment when superspin 3 equilibrates, then superdomains $2'$ and 3 coalesce; this happens with probability $\exp(-\tilde{d}_2')$. Otherwise, the leftmost up-spin in the segment freezes into a new superspin $3'$, and the process continues by iteration. It is clear that only superdomains of length $\tilde{d}>\tilde{d}_\mathrm{r}$ have been generated when the process

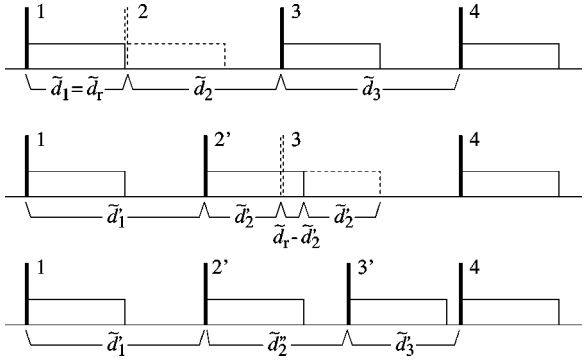

FIG. 5. Illustration of superdomain dynamics. Superspins are shown by the thin vertical rectangles; each has an equilibrated zone of length $\tilde{d}_r$ to its right, indicated by a horizontal rectangle. Shown is a situation where the relaxation time $\tilde{d}_r$ has just become equal to the smallest superdomain length, $\tilde{d}_1$. The equilibrated zone of superspin 1 then catches up with 2 and equilibrates this spin (first line). At this moment, there can be up-spins within the former equilibrated zone of 2; if there are, the leftmost of these becomes a new superspin $2'$, bounding a superdomain of length $\tilde{d}'_2$ (second line). If $\tilde{d}'_2<\tilde{d}_r$, the newly created equilibrated zone of $2'$ catches superspin 3. Within the zone of length $\tilde{d}'_2$ that is now no longer equilibrated (dashed) up-spins can again remain, with the leftmost becoming a new superspin $3'$. In the example, the relaxation process at $\tilde{d}_r$ stops at this point since $\tilde{d}'_3>\tilde{d}_r$; otherwise, it would continue in the same fashion.

terminates. One can thus now increase $\tilde{d}_r$ until the new minimum superdomain size is reached, at which point a new relaxation process as described above starts.

Above, we arrived at the superdomain model starting from the hypothesis of continuous time scale separation. The model lets us access, via an effective description, very low temperatures corresponding to extremely long relaxation times. By definition it is therefore difficult to demonstrate superdomain-type dynamics on the time scales of a numerical simulation. Nevertheless, the sample run at $\epsilon=0.02$ shown in Fig. 6 illustrates some important features of superdomain dynamics, in particular the regeneration of superspins and the resulting propagation of equilibrated zones.

To summarize the superdomain model, let us restate its dynamics. We present this in the form of a schematic simulation algorithm; a formal definition of the stochastic evolution of the sequence of superdomain lengths is, of course, possible but would be more awkward. We reemphasize that all lengths are *rescaled* lengths, $\tilde{d}=d\epsilon$.

1. Initialize superdomain lengths from an exponential distribution $P(\tilde{d})=\exp(-\tilde{d})$.

2. Set $\tilde{d}_r$ equal to the size of the smallest current superdomain. Let that size be $\tilde{d}_1$, with $\tilde{d}_2,\tilde{d}_3,\ldots,$ the sizes of the superdomains on the right. Set $i=1$.

3. Delete the now equilibrated superspin $i+1$. With probability $\exp(-\tilde{d}_i)$, the superdomains i and $i+1$ coalesce and the relaxation process at this $\tilde{d}_r$ is complete: let $\tilde{d}_i\leftarrow\tilde{d}_i+\tilde{d}_{i+1}$, delete superdomain $i+1$, and go back to step 2.

4. Otherwise, a new superspin $(i+1)'$ is created, a distance δ to the right of the old one which is distributed according to $P(\delta)\propto\exp(-\delta)$ over the range $\delta\in[\tilde{d}_r-\tilde{d}_i,\tilde{d}_r]$. This gives new superdomain lengths: $\tilde{d}_i\leftarrow\tilde{d}_i+\delta$ and $\tilde{d}_{i+1}\leftarrow\tilde{d}_{i+1}-\delta$. If $\tilde{d}_{i+1}\leqslant\tilde{d}_r$, increase $i\leftarrow i+1$, and go back to step 3. Otherwise the relaxation process at this $\tilde{d}_r$ is complete; go back to step 2.

Ideally, one would like to solve the above superdomain model directly and thus compute the dependence of the persistence function on $\tilde{d}_r$ analytically. The iterative process of superspin elimination and regeneration is difficult to keep track of, however, and we have not been able to find an analytical solution. Nevertheless, because the superdomain model expresses times in terms of the length scales $\tilde{d}_r$, which unlike the time scales themselves do not diverge for $T\to0$, it can be simulated easily and accurately; we have

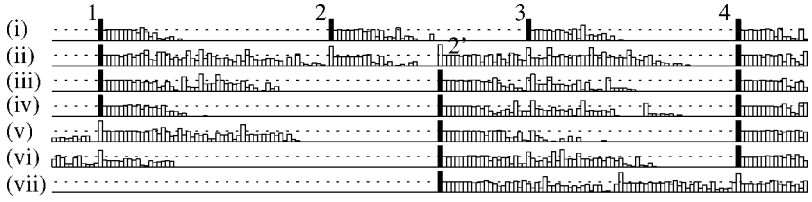

FIG. 6. A direct simulation run on a system at $\epsilon=0.02$ which provides support for the notion of superdomain-type dynamics. Shown is a section of 180 spins out of a much longer chain, for a single simulation run. The lines correspond to seven successive time intervals $[10^{10}a^{-7},10^{10}a^{-6}],\ldots,[10^{10}a^{-1},10^{10}a^{-0}]$, with $a=1.485$ so that the first interval begins at $10^{10}a^{-7}=6.26\times10^8$. (Geometrically increasing intervals were chosen because, from Eq. (42), relaxation time scales t_r are expected to increase very quickly with superdomain lengths $\tilde{d}_r$ for low T.) The boxes indicate the current magnetizations $\overline{s_i}$ of the spins, determined by averaging over the relevant time interval. A logarithmic scale is used, so that the highest boxes correspond to $\overline{s_i}=1$, the dashed lines to the equilibrium value $\overline{s_i}=c$, and the baselines to $\overline{s_i}=c^2$. (Lower values of $\overline{s_i}$ are not shown.) Filled boxes indicate spins that are persistently up over the entire time interval ($\overline{s_i}=1$). Note the similarity between the first two lines here and the superdomain dynamics sketched in Fig. 5: within the time interval (ii), the equilibrated zone of superspin 1 catches up with 2; a new superspin $(2')$ is created and eliminates superspin 3. Lines (v) and (vii) show events where superspins 1 and 4 are eliminated. Of course, ϵ here is still too large to be in the asymptotic limit $T\to0$ where superdomain dynamics applies exactly. This is why, in contrast to Fig. 5, the equilibrated zones of the superspins are not all of the same length, do not have sharply defined boundaries, and also do not increase perfectly monotonically in time.

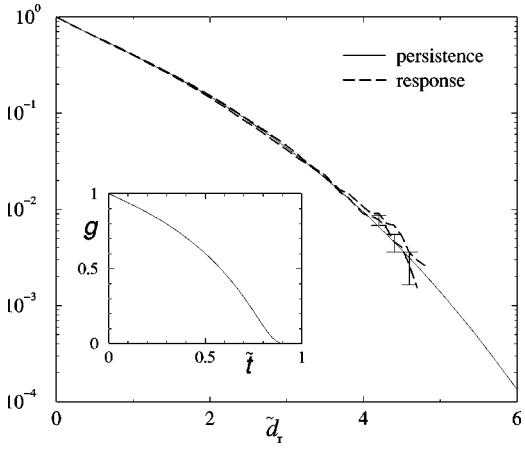

FIG. 7. Predictions of the superdomain model. Main plot, dashed lines: Response functions for $\epsilon_0/\epsilon=0.95$ and $\epsilon_0/\epsilon=1.05$ vs relaxation time $\tilde{d}_r$; on the latter, a few error bars are shown where they are significant. Solid lines: Persistence functions $\mathcal{P}_1$ and $\mathcal{P}_0$; the two lines are indistinguishable by eye. The inset shows the scaling function $g(\tilde{t})$ for the equilibrium relaxation functions, as derived from the superdomain persistence and the scaling function for the FPTs sketched in Fig. 4(a).

used systems of 10^5 superdomains (at $\tilde{d}_r=0$), checking that finite-size effects are negligible and typically averaging our results over 10^4 simulation runs.

The key quantity that we want to predict from the superdomain model is the persistence function. The up-spin persistence $\mathcal{P}_1$ is the fraction of up-spins that have never flipped since $\tilde{d}_r=0$. Since at $\tilde{d}_r=0$ all up-spins are superspins, $\mathcal{P}_1$ is the fraction of these initial superspins that have never been equilibrated. We show the results in Fig. 7; $\mathcal{P}_1$ initially decreases linearly with $\tilde{d}_r$, but then the decay becomes much faster and indeed superexponential in $\tilde{d}_r$.

If, as we have claimed, the superdomain model is the correct effective description for the $T\to 0$ dynamics of the East model, then it must obey the exact identity $\mathcal{P}_1=\mathcal{P}_0$ derived in Sec. IV A. $\mathcal{P}_0$ is measured in the superdomain model as the fraction of the chain which has never been swept by an equilibrated zone, a quantity that one might not have naively suspected to be connected to the number of persistent superspins. Nevertheless, our simulations show that indeed $\mathcal{P}_1=\mathcal{P}_0$ to very high accuracy ($\sim 1\%$, less than the relative error on the measurements of $\mathcal{P}_1$ and $\mathcal{P}_0$) in the superdomain model. In fact, both quantities are plotted in Fig. 7, but are indistinguishable by eye. This provides strong support for the correctness of the superdomain model; if, e.g., the mechanism for regenerating superdomains is neglected, one finds that the condition $\mathcal{P}_0=\mathcal{P}_1$ is violated.

A further consistency check on the model is obtained from the requirement that it should represent the *equilibrium* dynamics. The concentration of up-spins in the system, i.e., the magnetization $M=(1/L)\Sigma_i s_i$, should thus remain independent of $\tilde{d}_r$. Within the superdomain model, if there are N_s superspins at time $\tilde{d}_r$, one has

$$M=N_s(1+c\tilde{d}_r/\epsilon)/L\approx(N_s/L)(1+\tilde{d}_r) \tag{43}$$

since in addition to the superspins there are a further $cN_s\tilde{d}_r/\epsilon$ up-spins on the $N_s\tilde{d}_r/\epsilon$ sites covered by the equilibrated zones. This quantity should equal $M=c\approx\epsilon$ independently of $\tilde{d}_r$. Hence the average (rescaled) distance between superspins, $\epsilon L/N_s$, which is identical to the average superdomain length, must equal $1+\tilde{d}_r$ at time $\tilde{d}_r$. This is indeed what our simulations of the superdomain model show. One can push this comparison further and consider not just the total up-spin concentration, but the distribution of sizes of the domains formed by all spins (rather than just the superspins). This distribution must be a pure exponential, independently of $\tilde{d}_r$. It can be expressed in terms of the superdomain distribution by an appropriate convolution which accounts for the fact that additional up-spins exist in the equilibrated zones. Omitting the details, we only state that one finds in this way that the superdomain size distribution at time $\tilde{d}_r$ must be

$$P(\tilde{d};\tilde{d}_r)=\Theta(\tilde{d}-\tilde{d}_r)e^{-(\tilde{d}-\tilde{d}_r)}. \tag{44}$$

Again we find that this is verified in our simulations. Note that Eq. (44) has a simple intuitive interpretation: it corresponds to an exponential distribution of the segments of down-spins separating the equilibrated zone of each superdomain from the next superspin on the right.

A final check on the superdomain model is that it should obey FDT—since the original model obeys detailed balance, FDT is automatically satisfied but this is not guaranteed for the superdomain description. As explained in Sec. IV A, all nonlocal correlation (and hence response) functions vanish in the East model, so that one is free to consider either a local response of s_i to a local field or a response of the magnetization M to a uniform field h. Choosing the second option, the energy function is modified to $E=(1-h)\Sigma_i s_i$ which is equivalent to changing ϵ to $\epsilon'=\epsilon\exp(h/T)$ [or temperature from T to $T/(1-h)$]. The response to a field h switched on in the distant past and switched off at $t=0$ can thus be measured by initializing the system in an equilibrium state corresponding to ϵ' and monitoring the evolution of M during the subsequent dynamics at ϵ. By FDT this switch-off response should have the same time dependence as the correlation (and hence the persistence) functions. In the superdomain model, the measurement is performed by initializing the superdomains with a modified domain size distribution $P(\tilde{d})=(\epsilon'/\epsilon)\exp[-(\epsilon'/\epsilon)\tilde{d}]$ and then tracking the decay of the magnetization, measured as in Eq. (43), to its equilibrium value. The response functions simulated for $\epsilon'/\epsilon=0.95$ and 1.05 are plotted in Fig. 7 above, and show that the superdomain model indeed obeys FDT.

Pushing the above scenario further, one could consider nonlinear responses in the superdomain model, in particular a large ratio ϵ'/ϵ which corresponds to a quench to a much lower temperature. (For the superdomain model to remain applicable we still need $\epsilon'\ll 1$, of course.) The initial scaled domain lengths in the system are then of order $\epsilon/\epsilon'\ll 1$. In

the regime of small $\tilde{d}_r$ where these domain lengths are removed from the system, one sees that the probability $1-\exp(-\tilde{d}_r)\approx\tilde{d}_r$ of creating a new superspin is very small, tending to zero for $\tilde{d}_r\sim\epsilon/\epsilon'\to 0$. In this limit the superdomain dynamics becomes ''take the smallest superdomain and coalesce it with its neighbor on the right,'' which is precisely the paste-all model discussed in Sec. III D. While superdomain sizes remain $\ll 1$, the domain size distribution will thus be driven to the scaling distribution of the paste-all model. As demonstrated in Sec. III D, this scaling distribution is the *same* as that for the coarsening dynamics of the East model. Thus, the prediction of the superdomain model for the form of the domain size distribution, a long time after a quench from ϵ' to ϵ with $1\gg\epsilon'\gg\epsilon$, matches up precisely with that predicted in Sec. III C for a quench from $1\approx\epsilon'\gg\epsilon$. (Note that in the first case we are in principle talking about the *superdomain* size distribution, not the actual domain distribution as in Sec. III C. However, for small $\tilde{d}_r$ the two are identical since the number of up-spins within the equilibrated zones of the superdomains is negligible.)

Writing our result for the persistence function in the superdomain model (either $\mathcal{P}_1$ or $\mathcal{P}_0$, since they are identical) as $\mathcal{P}_{sd}(\tilde{d}_r)$, we can now translate it into a scaling prediction for the time dependence of the correlation and persistence functions at low T in the East model. Using the inverse of the scaling function $f(\tilde{d})$ from Eq. (42), one has

$$C(t)=\mathcal{P}_1(t)=\mathcal{P}_0(t)=\mathcal{P}_{sd}(f^{-1}(\tilde{t})),\quad \tilde{t}=\left(\frac{t}{t_*}\right)^{T\ln 2}. \tag{45}$$

Thus the relaxation functions show strong stretching, with the stretching exponent $T\ln 2$ decreasing to zero for $T\to 0$. However, the scaling function $g(\tilde{t})=\mathcal{P}_{sd}(f^{-1}(\tilde{t}))$ is nonexponential. In fact, since $f(\tilde{d})$ approaches a constant f_∞ for $\tilde{d}\to\infty$ as argued after Eq. (42), the scaling function in Eq. (45) decays to zero at a *finite* value $\tilde{t}=f_\infty$. On the basis of the results of Ref. [12] we would conjecture this value to be $f_\infty=1$, see below Eq. (42); the scaling function $g(\tilde{t})$ for this case is sketched in the inset of Fig. 7. It is important to bear in mind that the limit of $T\to 0$ considered here is taken at constant $\tilde{d}_r$ or, equivalently, constant $\tilde{t}$. If we look instead at fixed nonzero T then the relaxation functions are, of course, nonzero for all t, but this does not contradict $g(\tilde{t})$ dropping to zero at $\tilde{t}=f_\infty$. To see this, note that the asymptotic decay of all relaxation functions should be to leading order an exponential with the longest relaxation time, $\sim\exp(-t/t_*)$. This does remain nonzero for all t; but in terms of the scaled time $\tilde{t}$ it becomes $\sim\exp(-\tilde{t}^{1/T\ln 2})$ which converges to zero for $T\to 0$ at any fixed $\tilde{t}>1$.

We can now also come back to a point discussed at the end of Sec IV B: in principle the function $f(\tilde{d})$ may not be strictly monotonically increasing, but could instead be *constant* from a certain value $\tilde{d}_*$ onwards, $f(\tilde{d})=f_\infty$ for $\tilde{d}>\tilde{d}_*$. Looking at Eq. (45), however, this would lead to the conclusion that for any $\tilde{t}<f_\infty$ the relaxation functions are nonzero, approaching a nonzero limit as $\tilde{t}\to f_\infty$ but then dropping discontinuously to zero (in the limit $T\to 0$). This makes this hypothetical behavior of $f(\tilde{d})$ rather unlikely.

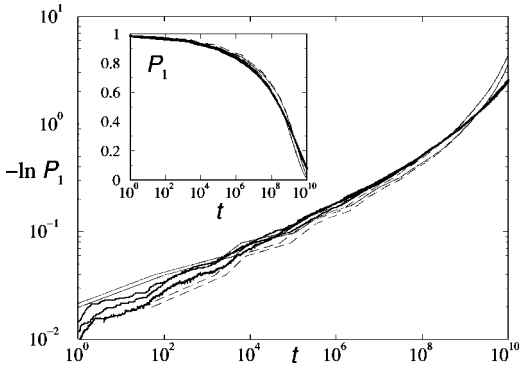

FIG. 8. Comparison of up-spin persistence function $\mathcal{P}_1$ from simulations with prediction of superdomain model, for $\epsilon=0.02$. A log-log plot of $-\ln\mathcal{P}_1(t)$ is shown, which would be straight for stretched exponential relaxation. The inset shows $\mathcal{P}_1(t)$ directly. Thick lines: $\mathcal{P}_1$ as simulated in three runs for a chain of length $L=2^{17}$; the correlation function $C(t)$ is also shown for one run but is indistinguishable from $\mathcal{P}_1(t)$ as predicted for low ϵ. Thin lines: Predictions of the superdomain model (see text). Dashed/solid: t determined from FPTs for up- and down-flips, respectively. Left/right curve of each pair: using mean of the log-FPT and the log of the MFPT, respectively.

As explained, one of the main benefits of the superdomain model is that it allows one to access very long time scales that diverge extremely quickly as T decreases. Since this is precisely the regime that is hard to probe with simulations, comparing the theoretical predictions with numerical data is not straightforward. We chose $\epsilon=0.02$, the lowest value for which we can simulate a significant part of the equilibrium relaxation. As Fig. 4 shows, the relation between rescaled FPTs $\tilde{\tau}$ and rescaled distances $\tilde{d}=\epsilon d$ has not yet reached its $\epsilon\to 0$ form, so it would make no sense to compare numerical data with superdomain predictions based on the latter. Instead, we use the numerically obtained FPTs to link time scales and length scales. In detail, we obtain for each unnormalized distance d the measured FPT, and plot against this time the superdomain model's persistence function $\mathcal{P}_{sd}(\tilde{d})$ at the relevant scaled distance $\tilde{d}=\epsilon d$. Since we measured FPT in four different ways—for up- and down-flips, and averaging FPTs or log FPTs—which we expect to become identical only for $T\to 0$, this procedure gives four slightly different curves for the superdomain predictions. As shown in Fig. 8, these bracket the numerically simulated up-spin persistence and correlation functions rather well, especially given that there are no fit parameters in the comparison. The largest deviations occur for large times, corresponding to large length scales. This is consistent with Fig. 4, which shows that in this regime the behavior still differs substantially from that expected in the limit $T\to 0$.

V. CONCLUSION

We have studied the dynamics of the East model. Consisting of uncoupled spins in a downward-pointing field, the

model has trivial equilibrium statistics. However, the kinetic constraint that spins can only flip if their left neighbor is up causes pronounced glassy features in the dynamics at low T, when the concentration of up-spins is low.

We first studied the nonequilibrium coarsening dynamics after a quench to low T. In the limit $\epsilon = \exp(-1/T) \to 0$ the equilibrium concentration of up-spins at the new temperature is negligible ($\approx \epsilon$) and the flipping down of up-spins becomes irreversible to leading order. This allows the dynamics to be described as coarsening via coalescence of down-spin domains. The process is hierarchical, being governed by a series of well-separated time scales. We solved this hierarchical coarsening dynamics exactly, using an independent intervals method that becomes exact for $T \to 0$. Anomalous coarsening results, with typical domain lengths scaling as $\overline{d} \sim t^{T \ln 2}$. The dominant divergence of the equilibration time for low T can also be estimated, and is given by the factor $t_* = \exp(1/T^2 \ln 2)$, an EITS dependence typical of fragile glasses. For large domain sizes $\overline{d}$ that are still small compared to the equilibrium value $\overline{d}_{\rm eq}$, the domain size distribution approaches a scaling form. We showed that this scaling distribution is equal to that of the paste-all model, and were able to define a whole family of interpolating models that all share this scaling distribution.

In the second part of the paper we focused on the equilibrium dynamics at low T. We showed that the standard relaxation functions, spin autocorrelation and persistence of up- and down-spins, become identical for $T \to 0$, so that only one of them needs to be considered. We then investigated the relation between time and length scales. Generalizing from the results in the coarsening regime $\tilde{d} = d/\overline{d}_{\rm eq} \ll 1$, we introduced a time scaling hypothesis. This implied that for $T \to 0$ one has continuous time scale separation, with domains of any two different scaled sizes $\tilde{d}$ relaxing on well-separated time scales. On this basis we proposed a model of superdomains, which are bounded by up-spins that are frozen on long time scales. The dynamics of this model is nontrivial and not, as yet, analytically tractable, but can easily be simulated since time is effectively measured in terms of the scaled distance $\tilde{d}$, whose relevant values remain $O(1)$ even for $T \to 0$. We verified that the model obeys important consistency requirements, in particular the equality of up-spin and down-spin persistence, the fluctuation-dissipation theorem, and the stationarity of up-spin concentration and domain size distribution in equilibrium.

From the superdomain model predictions we finally deduced that the equilibrium relaxation functions should decay for low T as $g(\tilde{t})$, with $g(\cdot)$ being a scaling function of $\tilde{t} = (t/t_*)^{T \ln 2}$. This demonstrates strong stretching for low T, but the overall relaxation is more complicated than a stretched exponential. In fact, the function $g(\cdot)$ decays faster than exponential, and in the limit $T \to 0$ at fixed $\tilde{t}$ reaches zero at a *finite* value of $\tilde{t}$. The lowest temperature T that we can conveniently simulate, corresponding to $\epsilon = 0.02$, is still rather far from the asymptotic $T \to 0$ limit but nevertheless showed reasonable agreement between numerical simulations and appropriately extracted predictions of the superdomain model. We would suggest that stretching but not simple stretched *exponential* behavior may be rather generic in glassy dynamics. Actual stretched exponentials could more often than not be just convenient fitting functions over a limited number of decades in time. To clarify this point, a study of low-temperature relaxation in other solvable models exhibiting glassy dynamics would obviously be desirable.

In future work, it would be interesting to see whether the out-of-equilibrium response of spins to a local field could also be analyzed within the irreversible coarsening framework we used above. This response function was simulated in Ref. [22] and found there to be monotonic; at lower T, however, nonmonotonicities should appear according to a later conjecture [29]. A closer investigation of out-of-equilibrium FDT relations would also be worthwhile. Previous results for these [22] have to be regarded with some caution since they were constructed using a disconnected correlator; see, e.g., Ref. [39] for a discussion of this point. Finally, as regards the equilibrium dynamics, it will be interesting to analyze the implications of the superdomain description for dynamic heterogeneities, making a connection to the recent work of Garrahan and Chandler [20].

ACKNOWLEDGMENT

P.S. acknowledges financial support through Nuffield Grant No. NAL/00361/G.

[1] J. Jäckle, Rep. Prog. Phys. **49**, 171 (1986).
[2] C.A. Angell, Science **267**, 1924 (1995).
[3] M.D. Ediger, C.A. Angell, and S.R. Nagel, J. Phys. Chem. **100**, 13 200 (1996).
[4] P.G. Debenedetti, *Metastable Liquids: Concepts and Principles* (Princeton University Press, Princeton, 1996).
[5] J.P. Bouchaud, L.F. Cugliandolo, J. Kurchan, and M. Mézard, in *Spin Glasses and Random Fields*, edited by A.P. Young (World Scientific, Singapore, 1998), pp. 161–223.
[6] G. Adam and J.H. Gibbs, J. Chem. Phys. **43**, 139 (1965).
[7] R. Richert and H. Bässler, J. Phys.: Condens. Matter **2**, 2273 (1990).
[8] R.G. Palmer, D.L. Stein, E. Abrahams, and P.W. Anderson, Phys. Rev. Lett. **53**, 958 (1984).
[9] G.H. Fredrickson and H.C. Andersen, Phys. Rev. Lett. **53**, 1244 (1984).
[10] F. Ritort and P. Sollich, Adv. Phys. **52**, 219 (2003).
[11] J. Jäckle and S. Eisinger, Z. Phys. B: Condens. Matter **84**, 115 (1991).
[12] D. Aldous and P. Diaconis, J. Stat. Phys. **107**, 945 (2002).
[13] S. Eisinger and J. Jäckle, J. Stat. Phys. **73**, 643 (1993).
[14] S.J. Pitts and H.C. Andersen, J. Chem. Phys. **114**, 1101 (2001).
[15] K. Kawasaki, Physica A **215**, 61 (1995).
[16] S.J. Pitts, T. Young, and H.C. Andersen, J. Chem. Phys. **113**,

8671 (2000).
[17] P. Sollich and M.R. Evans, Phys. Rev. Lett. **83**, 3238 (1999).
[18] A. Buhot and J.P. Garrahan, Phys. Rev. E **64**, 021505 (2001).
[19] A. Buhot and J.P. Garrahan, J. Phys.: Condens. Matter **14**, 1499 (2002).
[20] J.P. Garrahan and D. Chandler, Phys. Rev. Lett. **89**, 035704 (2002).
[21] M.A. Muñoz, A. Gabrielli, H. Inaoka, and L. Pietronero, Phys. Rev. E **57**, 4354 (1998).
[22] A. Crisanti, F. Ritort, A. Rocco, and M. Sellitto, J. Chem. Phys. **113**, 10 615 (2000).
[23] G. De Smedt, C. Godrèche, and J.M. Luck, Eur. Phys. J. B **27**, 363 (2002).
[24] E. Follana and F. Ritort, Phys. Rev. B **54**, 930 (1996).
[25] M. Schulz and S. Trimper, Int. J. Mod. Phys. B **11**, 2927 (1997).
[26] J. Berg, S. Franz, and M. Sellitto, Eur. Phys. J. B **26**, 349 (2002).
[27] S.M. Fielding, Phys. Rev. E **66**, 016103 (2002).
[28] M.E.J. Newman and C. Moore, Phys. Rev. E **60**, 5068 (1999).
[29] J.P. Garrahan and M.E.J. Newman, Phys. Rev. E **62**, 7670 (2000).
[30] J.P. Garrahan, J. Phys.: Condens. Matter **14**, 1571 (2002).
[31] B. Derrida, C. Godrèche, and I. Yekutieli, Phys. Rev. A **44**, 6241 (1991).
[32] A.B. Bortz, M.H. Kalos, and J.L. Lebowitz, J. Comput. Phys. **17**, 10 (1975).
[33] What we mean by irreversibility to leading order is that, although down-spins do flip back up during the relaxation processes that cause the domain coarsening, they have a negligibly small probability of being up in a snapshot at some randomly chosen time.
[34] A.J. Bray, B. Derrida, and C. Godrèche, Europhys. Lett. **27**, 175 (1994).
[35] F. Mauch and J. Jäckle, Physica A **262**, 98 (1999).
[36] F. Chung, P. Diaconis, and R. Graham, Adv. Appl. Math. **27**, 192 (2001).
[37] Already for $d=4$ one finds by explicit diagonalization of the master operator that there are two distinct eigenvalues scaling with the highest power of ϵ, $\epsilon^2/4$, and $2\epsilon^2/3$. In Ref. [35] it was shown for $d=4$ (and conjectured for all $d=2^k$) that in finite chains of length d nevertheless only *one* of these smallest eigenvalues $\sim\epsilon^k$ contributes to the decay of the equilibrium correlation function. A similar result should hold for the *survival probability* of an up-spin at distance $d=2^k$, but for other values of d it seems likely that several of the eigenvalues scaling with the highest power of ϵ would contribute. This is because for such d there can be a number of different relaxation paths of minimal height, whereas for $d=2^k$ there is only one such path.
[38] J. Jäckle and D. Sappelt, Physica A **192**, 691 (1993).
[39] P. Sollich, S. Fielding, and P. Mayer, J. Phys.: Condens. Matter **14**, 1683 (2002).